Quantum optics with quantum gases: Controlled state reduction by designed light scattering

Igor B. Mekhov[1,2,*] and Helmut Ritsch[1]
[1]*Institute for Theoretical Physics, University of Innsbruck, Technikerstraße 25, 6020 Innsbruck, Austria*
[2]*Faculty of Physics, St. Petersburg State University, Ulianovskaya 1, 198504 St. Petersburg, Russia*
(Received 27 April 2009; published 7 July 2009)

Cavity-enhanced light scattering from an ultracold gas in an optical lattice constitutes a quantum measurement with a controllable form of the measurement backaction. Time-resolved counting of scattered photons alters the state of the atoms without particle loss implementing a quantum nondemolition measurement. The conditional dynamics is given by the interplay between photodetection events (quantum jumps) and no-count processes. The class of emerging atomic many-body states can be chosen via the optical geometry and light frequencies. Light detection along the angle of a diffraction maximum (Bragg angle) creates an atom-number-squeezed state, while light detection at diffraction minima leads to the macroscopic superposition states (Schrödinger cat states) of different atom numbers in the cavity mode. A measurement of the cavity transmission intensity can lead to atom-number-squeezed or macroscopic superposition states depending on its outcome. We analyze the robustness of the superposition with respect to missed counts and find that a transmission measurement yields more robust and controllable superposition states than the ones obtained by scattering at a diffraction minimum.

DOI: 10.1103/PhysRevA.80.013604 PACS number(s): 03.75.Lm, 42.50.−p, 05.30.Jp

I. INTRODUCTION

Both quantum optics and physics of ultracold quantum gases currently represent the well-established and actively developing field of modern quantum science [1,2]. However, the interaction between the two fields is far from being close.

Historically, classical optics, treating light as classical electromagnetic waves, has become one of the most developed and fruitful fields of physics. It has provided us with many technological breakthroughs, e.g., the highest level of measurement precision. Quantum optics, which considers the light as quantum particles (photons), thus going beyond the mean-field (classical) description of the electromagnetic waves, currently is also a well-developed field both theoretically and experimentally [3].

The progress in laser cooling techniques in the last decades of the 20th century led to the foundation of a new field of atom physics: atom optics. It was shown that the matter waves of ultracold atoms can be treated similar to light waves in classical optics and can be manipulated using the forces and potentials of laser light beams. The quantum properties of matter waves beyond the mean-field description became accessible after 1995, when the first Bose-Einstein condensate (BEC) and many other fascination quantum states of bosonic and fermionic ultracold atoms were obtained [1,2]. An exciting demonstration of "quantum atom optics" was presented in 2002, when the quantum phase transition between two states of atoms with nearly the same mean density but radically different quantum fluctuations was obtained: superfluid (SF) to Mott insulator (MI) state transition [4,5].

The roles of light and matter in optics and atom optics are completely reversed. Various devices known in optics such as beam splitters, mirrors, diffraction grating, etc., are created using light forces and applied for matter waves. However, up to now, the absolute majority of even very involved setups and theoretical models of quantum atom optics treats light as an essentially classical axillary tool to prepare and probe intriguing atomic states. In these contexts, the periodic micropotentials of light (optical lattices) play the role of cavities in optics enabling one to store and manipulate various atomic quantum states.

Quantum optics with quantum gases should close the gap between quantum optics and atom optics by addressing phenomena, where the quantum natures of both light and matter play equally important role. Experimentally, such an ultimate quantum level of the light-matter interaction became feasible only recently, when the quantum gas was coupled to the mode of a high-Q cavity [6–9]. Even early theoretical works on scattering of quantized light from a BEC was not realized so far [10–22]. However, it is cavity quantum electrodynamics (QED) with quantum gases that will provide the best interplay between the atom- and light-stimulated quantum effects.

On one hand, the quantum properties of atoms will manifest themselves in the scattered light, which will lead to novel nondestructive methods of probing and manipulating atomic states by light measurement [23–35]. On the other hand, the quantization of light (i.e., trapping potentials) will modify atomic many-body dynamics well known only for classical potentials and give rise to novel quantum phases [36–43]. This paper addresses the first problem.

In this work, we will extend our treatment of the detection of light scattered from ultracold atoms in optical lattices presented in Ref. [26], where the quantum measurement of light was considered as a method to prepare particular quantum states of atoms thanks to the measurement backaction. Except detailing the theoretical approach, we will consider a different optical configuration of the measurement process: cavity transmission spectroscopy instead of light scattering. As we will show, it turns out that such a configuration will allow us much better control and flexibility in atomic state preparation. This is in particular true for the preparation of

*igor.mekhov@uibk.ac.at

macroscopic superposition states (known as Schrödinger cat states), which can be more robust in comparison to those considered before [26,40].

We will show that detecting the light scattered from ultracold atoms in an optical lattice enables one to prepare various types of the atom-number-squeezed and macroscopic superposition states. An important point is that the type of the state and its properties strongly depend on the optical geometry. Varying the optical parameters (angles between the laser beams and lattice atoms, light frequencies, or lattice period) one can prepare various quantum states of ultracold atoms. Moreover, as the optical measurement is nondestructive, in the sense of the quantum nondemolition (QND) measurements, one can make sequential measurements on the same sample without completely destroying its quantum properties.

Generalizing the methods developed for spin squeezing in thermal atomic ensembles [44–48] for the case of light scattering from ultracold quantum gases will enable ones to reach the unprecedented level of the measurement precision, which is required, e.g., for atomic clocks and the detection of gravitational waves.

The paper is organized as follows. In Sec. II, a general theoretical model is formulated, which, in Sec. III, is extended to the quantum backaction of the light measurement on the atomic state. Section IV is devoted to the scattering of the transverse probe in to the cavity. In Sec. V, the properties of photon statistics are analyzed. The state preparation by the cavity transmission measurement is discussed in Sec. VI. The robustness of the macroscopic superposition states is analyzed in Sec. VII. The main results are summarized in Sec. VIII.

II. GENERAL MODEL

We consider N ultracold atoms trapped in a periodic optical lattice potential with M sites. In addition to the strong trapping beams, a subset of K sites, with $K \leq M$, is illuminated by a weak probe at some angle to the lattice atoms. The scattered light is collected by a cavity. The photons leaking out of the cavity are counted then with a photodetector. The schematic setup is shown in Fig. 1, where, for simplicity, the trapping beams are not shown. In general, the setup is not restricted by a simplified scheme in Fig. 1: the lattice can be one, two, or three dimensional; the probe and cavity modes can be standing or traveling waves or they can be even formed by two different modes of the same cavity. K illuminated sites can be selected in some nontrivial way, e.g., each second lattice site can be illuminated by choosing the probe wavelength two times larger than the lattice period. In addition to the external probe, a probing through a cavity mirror will be considered.

The main goal of this paper is to study how the measurement of the photons leaking out of the cavity will affect the quantum state of the ultracold atoms. Such a measurement backaction is possible due to the entanglement between light and matter, which develops during the interaction process. According to quantum mechanics, in the presence of th e entanglement, the measurement of one of the quantum subsystems (light) will also affect another quantum subsystem (atoms).

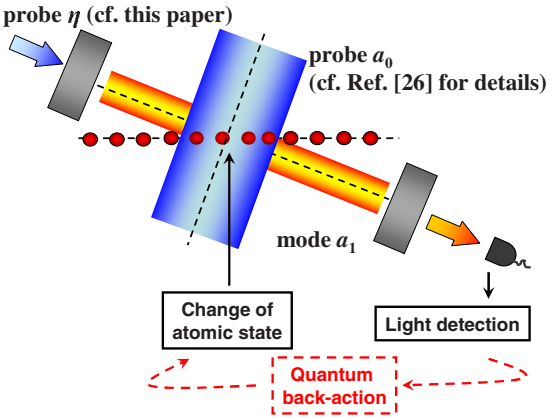

FIG. 1. (Color online) Setup. A lattice is illuminated by the transverse probe a_0 and probe through a mirror η. The photodetector measures photons leaking the cavity. Due to the quantum backaction, the light measurement leads to the modification of the atomic quantum state.

We will use the physical model presented in details in Ref. [25]. The theoretical formulation starts with a generalized Bose-Hubbard model including the quantization of light. As here, unlike Ref. [49], the far off-resonant light scattering will be considered, the role of the atomic excited states is not important, and they can be adiabatically eliminated from the dynamics. As will be focused here on the quantum measurement process, it is reasonable to neglect several processes that have been considered in other works [37,40,41] to avoid the complications. One of such processes to be neglected is the details of atomic dynamics. The tunneling of atoms in the lattice potential plays indeed an important role in establishing a particular quantum atomic state. However, after the state is established, one can assume that the scattering of the probe occurs on the time scale faster than slow tunneling. Thus, from the light-scattering point of view, the atomic distribution can be considered frozen and the tunneling is not important. It is especially reasonable to neglect the tunneling dynamics in this paper because we will show that even after that rather obvious dynamics is neglected, there is still nontrivial dynamics (quantum jumps) exclusively associated with the quantum measurement process, which is the main subject of our present work.

After those simplifications, the Hamiltonian of the problem takes the form,

$$H = \hbar(\omega_1 + U_{11}\hat{D}_{11})a_1^\dagger a_1 + \hbar U_{10}(\hat{D}_{10}^* a_0^* a_1 + \hat{D}_{10} a_0 a_1^\dagger) - i\hbar(\eta^* a_1 - \eta a_1^\dagger), \quad (1)$$

where a_1 is the cavity-mode annihilation operator of the frequency ω_1. The external probe of the frequency ω_p is assumed to be in a coherent state; thus, its amplitude is given by a c number a_0. The spatial mode functions of the probe and cavity modes are $u_{1,0}(\mathbf{r})$. $U_{lm} = g_l g_m / \Delta_a$ $(l,m = 0,1)$, where $g_{1,0}$ are the atom-light coupling constants, $\Delta_a = \omega_1 - \omega_a$ is the cavity-atom detuning, and η is the amplitude of the additional probing through a mirror at the frequency ω_p.

We assumed the probe-cavity detuning $\Delta_p=\omega_p-\omega_1 \ll \Delta_a$. The operators $\hat{D}_{lm}=\Sigma_{j=1}^{K} u_l^*(\mathbf{r}_j)u_m(\mathbf{r}_j)\hat{n}_j$ sum contributions from all illuminated sites with the atom-number operators $\hat{n}_j$ at the position $\mathbf{r}_j$.

The first term in Eq. (1) describes the atom-induced shift of the cavity resonance. The second one reflects scattering (diffraction) of the probe a_0 into a cavity mode a_1. For a quantum gas, the frequency shift and probe-cavity coupling coefficient are operators, which leads to different light scattering from various atomic quantum states [23–25,27].

The Hamiltonian (1) describes QND measurements of the variables related to $\hat{D}_{lm}$ measuring the photon number $a_1^\dagger a_1$, as the criteria for the QND measurements are fulfilled [50]. Note that one has a QND access to various many-body variables, as $\hat{D}_{lm}$ strongly depend on the lattice and light geometry via $u_{0,1}(\mathbf{r})$. This is an advantage of the lattice comparing to single- or double-well setups, where the photon measurement backaction was considered [51–54]. Moreover, such a geometrical approach can be extended to other quantum arrays, e.g., ion strings [55].

For example, one can consider a one-dimensional lattice of the period d with atoms trapped at $x_j=jd(j=1,2,\ldots,M)$. In this case, the geometric mode functions can be expressed as follows: $u_{0,1}(\mathbf{r}_j)=\exp(ijk_{0,1x}d+\phi_{0,1j})$ for traveling waves, and $u_{0,1}(\mathbf{r}_j)=\cos(jk_{0,1x}d+\phi_{0,1j})$ for standing waves, where $k_{0,1x}=|\mathbf{k}_{0,1}|\sin\theta_{0,1}$, $\theta_{0,1}$ are the angles between mode wave vectors $\mathbf{k}_{0,1}$ and a vector normal to the lattice axis. In the plane-wave approximation, additional phases $\phi_{0,1j}$ are j independent. The general angular distributions of light scattered from ultracold atoms in optical lattices were presented in Refs. [23,25,27].

For some geometries, $\hat{D}_{11}$ can reduce to the operator $\hat{N}_K=\Sigma_{j=1}^{K}\hat{n}_j$ of the atom number at K sites [23–25] (if a_1 is a traveling wave at an arbitrary angle to the lattice or the standing wave with atoms trapped at the antinodes). If the probe and cavity modes are coupled at a diffraction maximum (Bragg angle), i.e., all atoms scatter light in phase, $u_1^*(\mathbf{r}_j)u_0(\mathbf{r}_j)=1$, the probe-cavity coupling is maximized, and $\hat{D}_{10}=\hat{N}_K$. If they are coupled at a diffraction minimum, i.e., the neighboring atoms scatter out of phase, $\hat{D}_{10}=\Sigma_{j=1}^{K}(-1)^{j+1}\hat{n}_j$ is the operator of the number difference between odd and even sites. Thus, the atom number as well as number difference can be nondestructively measured. Note that those are just two of the many examples of how a QND variable and thus the projected state can be chosen by the geometry.

III. MEASUREMENT BACKACTION

In this section, we present the solution for the quantum state of the coupled light-matter system including the measurement process. Importantly, it is possible to obtain an analytical solution with a very transparent physical meaning thanks to the approximations used (slow tunneling and coherent state of the external probes).

The initial motional state of the ultracold atoms trapped in the periodic lattice potential at the time moment $t=0$ can be represented as

$$|\Psi^a(0)\rangle=\sum_q c_q^0|q_1,\ldots,q_M\rangle, \tag{2}$$

which is a quantum superposition of the Fock states corresponding to all possible classical configurations $q=\{q_1,\ldots,q_M\}$ of N atoms at M sites, where q_j is the atom number at the site j. For each classical configuration q, the total atom number is conserved: $\Sigma_j^M q_j=N$. This superposition displays the uncertainty principle, stating that at ultralow temperatures even a single atom can be delocalized in space, i.e., there is a probability to find an atom at any lattice site. We will show how this atomic uncertainty is influenced by the light detection.

For example, for a limiting case of the MI state, where the atom numbers at each lattice site are precisely known, only one Fock state will exist in Eq. (2): $|\Psi_{\mathrm{MI}}\rangle=|1,1,\ldots,1\rangle$ for the MI with one atom at each site. On the other hand, the SF state is given by the superposition of all possible classical configurations with multinomial coefficients,

$$|\Psi_{\mathrm{SF}}^a\rangle=\frac{1}{(\sqrt{M})^N}\sum_q\sqrt{\frac{N!}{q_1!\,q_2!\,\ldots q_M!}}|q_1,q_2,\ldots,q_M\rangle. \tag{3}$$

Thus, the atom number at a single site as well as the atom number at $K<M$ sites is uncertain in the SF state.

As an initial condition, we assume that at the time moment $t=0$ the light and matter are disentangled, and the initial state of light is a coherent state with the amplitude α_0. Thus, the initial quantum state of the system is given by the product state $|\Psi(0)\rangle=|\Psi^a(0)\rangle|\alpha_0\rangle$. In particular, initially, the light can be in the vacuum state $|0\rangle$.

We use the open system approach [56] to describe the continuous counting of the photons leaking out the cavity of the cavity decay rate κ. According to that approach, when the photon is detected at the moment t_i, the quantum jump occurs, and the state instantaneously changes to a new one obtained by applying the cavity photon annihilation operator $|\Psi_c(t_i)\rangle\rightarrow a_1|\Psi_c(t_i)\rangle$ and renormalization (the subscript c underlines that we deal with the state conditioned on the photocount event). Between the photocounts, the system evolves with a non-Hermitian Hamiltonian $H-i\hbar\kappa a_1^\dagger a_1$. Such an evolution gives a quantum trajectory for $|\Psi_c(t)\rangle$ conditioned on the detection of photons at times $t_1,t_2,\ldots$. The probability of the photon escape within the time interval t is $2\kappa t\langle a_1^\dagger a_1\rangle_c$, where $\langle a_1^\dagger a_1\rangle_c$ is the conditional photon number in the cavity, i.e., the photon number calculated for the conditional quantum state $|\Psi_c(t)\rangle$.

The state $|\Psi_c(t)\rangle$ should be found by solving the Schrödinger equation with the non-Hermitian Hamiltonian for no-count intervals and applying the jump operator a_1 at the moments of photocounts. Thanks to the slow tunneling approximation, the Hamiltonian (1) does not mix the Fock states in expression (2). So, the problem is significantly reduced to separate finding solutions for each classical atomic configuration $q=\{q_1,\ldots,q_M\}$, after that the full solution will be given by the superposition of those solutions.

The next simplification appears thanks to the use of the external probes in the coherent state. It is known [57,58] that,

if a coherent probe illuminates a classical atomic configuration q in a cavity, the light remains in a coherent state, however, with some prefactor $\exp[\Phi_q(t)]|\alpha_q(t)\rangle$. The prefactor is indeed not important for a single classical configuration as it disappears after the renormalization, but it will play a role, when the superposition of classical solutions with different prefactors will be considered. Moreover, the light amplitude $\alpha_q(t)$ is simply given by the solution of a classical Maxwell's equation,

$$\alpha_q(t) = \frac{\tilde{\eta} - iU_{10}\tilde{a}_0 D_{10}^q}{i(U_{11}D_{11}^q - \Delta_p) + \kappa} e^{-i\omega_p t} + \left(\alpha_0 - \frac{\tilde{\eta} - iU_{10}\tilde{a}_0 D_{10}^q}{i(U_{11}D_{11}^q - \Delta_p) + \kappa}\right) e^{-i(\omega_1 + U_{11}D_{11}^q)t - \kappa t}, \tag{4}$$

where we introduced the constant probe amplitudes $\tilde{a}_0$ and $\tilde{\eta}$ as $a_0 = \tilde{a}_0 \exp(-i\omega_p t)$ and $\eta = \tilde{\eta}\exp(-i\omega_p t)$; $D_{lm}^q = \Sigma_{j=1}^K u_l^*(\mathbf{r}_j)u_m(\mathbf{r}_j)q_j$ is a realization of the operator $\hat{D}_{lm}$ at the configuration $q=\{q_1,\ldots,q_M\}$. As in classical optics, the first term in Eq. (4) gives the oscillations at the probe frequency, while the second term gives the transient process with the oscillations at the cavity frequency shifted by the dispersion $\omega_1 + U_{11}D_{11}^q$, which decays with the rate κ. In the following, we introduce the slowly varying light amplitude $\tilde{\alpha}_q(t)$ as $\alpha_q(t) = \tilde{\alpha}_q(t)\exp(-i\omega_p t)$ and, for the notation simplicity, we will drop the tilde sign in all amplitudes $\tilde{a}_0$, $\tilde{\eta}$, and $\tilde{\alpha}_q(t)$.

The function $\Phi_q(t)$ in the prefactor is a complex one and is given by

$$\Phi_q(t) = \int_0^t \left[\frac{1}{2}(\eta\alpha_q^* - iU_{10}a_0 D_{10}^q \alpha_q^* - \text{c.c.}) - \kappa|\alpha_q|^2\right] dt, \tag{5}$$

where the light amplitude $\alpha_q(t)$ is given by Eq. (4).

First, let us consider the solution for the atomic state initially containing a single Fock state $|q_1,\ldots,q_M\rangle$. The solution for light is given by the solution for the classical configuration $q=\{q_1,\ldots,q_M\}$. So, the evolution is given by the product state $|q_1,\ldots,q_M\rangle|\alpha_q(t)\rangle$. An important property of this solution is that a quantum jump does not change the state since applying the jump operator a_1 simply leads to the prefactor $\alpha_q(t)$, which disappears after the renormalization. Therefore, even in the presence of photocounts (i.e., quantum jumps), the time evolution is continuous and is given by Eq. (4): after a transient process for $t < 1/\kappa$, the steady state for $\alpha_q(t)$ is achieved. Note that in contrast to many problems in quantum optics [56], where the steady state is a result of averaging over many quantum trajectory, here, the steady state appears even at a single-quantum trajectory for $t > 1/\kappa$. This is a particular property of the coherent quantum state. The continuity of evolution of the state $|q_1,\ldots,q_M\rangle|\alpha_q(t)\rangle$, and, hence, more generally, the un-normalized state including the prefactor $\exp[\Phi_q(t)]|q_1,\ldots,q_M\rangle|\alpha_q(t)\rangle$, independently of the presence of the quantum jumps provides us a significant mathematical simplification. Moreover, we will use the result that after the time $t > 1/\kappa$; all light amplitudes α_q are constant for all Fock states $|q_1,\ldots,q_M\rangle$.

Let us now consider the full initial state given by superposition (2). As stated, the evolution of each term is independent and contains the continuous part $\exp[\Phi_q(t)]|q_1,\ldots,q_M\rangle|\alpha_q(t)\rangle$. Thus, applying the jump operators at the times of the photodetections $t_1,t_2,\ldots,t_m$ leads to the following analytical solution for the conditional quantum state at the time t after m photocounts:

$$|\Psi_c(m,t)\rangle = \frac{1}{F(t)}\sum_q \alpha_q(t_1)\alpha_q(t_2)\ldots\alpha_q(t_m)e^{\Phi_q(t)}c_q^0|q_1,\ldots,q_M\rangle \times|\alpha_q(t)\rangle, \tag{6}$$

where

$$F(t) = \sqrt{\sum_q |\alpha_q(t_1)|^2|\alpha_q(t_2)|^2,\ldots,|\alpha_q(t_m)|^2|e^{\Phi_q(t)}|^2|c_q^0|^2}$$

is the normalization coefficient.

In contrast to a single atomic Fock state, solution (6), in general, is not factorizable into a product of the atomic and light states. Thus, in general, the light and matter are entangled. Moreover, in contrast to a single Fock state, the quantum jump (applying a_1) changes the state, and the evolution of the full $|\Psi_c(m,t)\rangle$ is not continuous.

The general solution (6) valid for all times simplifies significantly for $t > 1/\kappa$, when all α_q are constants, and if the first photocount occurred at $t_1 > 1/\kappa$, when all α_q has already become constants. The latter assumption is especially probable for the small cavity photon number since the probability of the photon escape within the time interval t is $2\kappa t\langle a_1^\dagger a_1\rangle_c$. This solution takes the form

$$|\Psi_c(m,t)\rangle = \frac{1}{F(t)}\sum_q \alpha_q^m e^{\Phi_q(t)}c_q^0|q_1,\ldots,q_M\rangle|\alpha_q\rangle, \tag{7}$$

$$\alpha_q = \frac{\eta - iU_{10}a_0 D_{10}^q}{i(U_{11}D_{11}^q - \Delta_p) + \kappa}, \tag{8}$$

$$\Phi_q(t) = -|\alpha_q|^2\kappa t + (\eta\alpha_q^* - iU_{10}a_0 D_{10}^q\alpha_q^* - \text{c.c.})t/2, \tag{9}$$

with the normalization coefficient

$$F(t) = \sqrt{\sum_q |\alpha_q|^{2m}e^{-2|\alpha_q|^2\kappa t}|c_q^0|^2}.$$

The solution (7) does not depend on the photocount times $t_1,t_2,\ldots,t_m$ any more. Note however, that even for $t > 1/\kappa$, when all α_q reached their steady states and are constants, solution (7) is still time dependent. Thus, the time $t = 1/\kappa$ is not a characteristic time scale for the steady state of the full solutions (6) and (7). The stationary light amplitudes α_q in Eq. (8) are given by the Lorentz functions in the absolute correspondence with classical optics. The function $\Phi_q(t)$ has also simplified and contains the first real term responsible for the amplitudes of the coefficients in the quantum superposition and the second imaginary term responsible for their phases.

The solutions (6) and (7) show how the probability to find the atomic Fock state $|q_1,\ldots,q_M\rangle$ (corresponding to the classical configuration q) changes in time. Such a change in the atomic quantum state appears essentially due to the measurement of photons and is a direct consequence of the light-matter entanglement. According to quantum mechanics, by measuring one of the entangled subsystem (light) one also affects the state of another subsystem (atoms). Now we can focus on that purely measurement-base dynamics since other obvious sources of the time evolution (e.g., tunneling) we neglected in our model. The initial probability to find the Fock state $|q_1,\ldots,q_M\rangle$ is $p_q(0)=|c_q^0|^2$. From Eq. (6), the time evolution of this probability is given by

$$p_q(m,t)=|\alpha_q(t_1)|^2|\alpha_q(t_2)|^2,\ldots,|\alpha_q(t_m)|^2|e^{\Phi_q(t)}|^2p_q(0)/F^2(t). \tag{10}$$

For $t,t_1>1/\kappa$ [cf. Eq. (7)], it reduces to

$$p_q(m,t)=|\alpha_q|^{2m}e^{-2|\alpha_q|^2\kappa t}p_q(0)/F^2(t). \tag{11}$$

In the following, we will demonstrate the applications of the general solutions (6) and (7) in the examples, where, for simplicity, only a single statistical quantity is important, instead of the whole set of all possible configurations q. As particular examples, we will consider the cases, where that statistical quantity (let us now call it z) is the atom number at K lattice sites or the atom-number difference between odd and even sites. Thus, instead of the huge number of detailed probabilities $p_q(m,t)$, we will be interested in the probability $p(z,m,t)$ to find a particular value of z. For the initial state (2) at $t=0$, $p_0(z)=\Sigma_{q'}|c_{q'}^0|^2$ with the summation over all configurations q' having the same z. As under our assumptions all light amplitudes $\alpha_q(t)$ depend only on z, we change their subscript to z and write the probability to find a particular value of z at time t after m photocounts,

$$p(z,m,t)=|\alpha_z(t_1)|^2|\alpha_z(t_2)|^2,\ldots,|\alpha_z(t_m)|^2e^{2\,\mathrm{Re}\,\Phi_z(t)}p_0(z)/F^2(t), \tag{12}$$

For $t,t_1>1/\kappa$, it reduces to

$$p(z,m,t)=|\alpha_z|^{2m}e^{-2|\alpha_z|^2\kappa t}p_0(z)/F^2(t),$$

$$F(t)=\sqrt{\sum_z|\alpha_z|^{2m}e^{-2|\alpha_z|^2\kappa t}p_0(z)}. \tag{13}$$

In the following we will consider solution (7). When the time progresses, both m and t increase with an essentially probabilistic relation between them. The quantum Monte Carlo method [56] establishes such a relation, thus, giving a quantum trajectory. Note that thanks to the simple analytical solution (7), the method gets extremely simple. The evolution is split into small time intervals δt_i. In each time step, the conditional photon number is calculated in state (7), and the probability of the photocount within this time interval $2\kappa\langle a_1^\dagger a_1\rangle_c\delta t_i$ is compared with a random number $0<\epsilon_i<1$ generated in advance, thus, deciding whether the detection (if $2\kappa\langle a_1^\dagger a_1\rangle_c\delta t_i>\epsilon_i$) or no-count process (otherwise) has happened.

IV. TRANSVERSE PROBING

In this section, we will consider a case, where only the transverse probe a_0 is present, while the probe through the mirror does not exist, $\eta=0$. We presented this situation in the previous letter [26]. Here, we remind the most important results and underline the difficulties in the state preparation using the transverse probing. In Sec. VI, we will switch to a new geometry, probing through a mirror, and will show that such geometry contains the features similar to the transverse probing but is more flexible and enables us to solve the difficulties associated with the transverse probing scheme.

In this section, we neglect the dispersive frequency shift assuming that $U_{11}D_{11}^q\ll\kappa$ or Δ_p. Thus, the light amplitudes α_q will only depend on the quantity D_{10}^q. In Sec. VI, in contrast, we will focus on the case, where the dispersive mode shift is very important.

A. Preparation of the atom-number-squeezed states

The measurement of photons scattered in the direction of a diffraction maximum (Bragg angle) leads to a preparation of a state with the reduced (squeezed) fluctuations of the atom number at the lattice region with K illuminated sites [26]. The condition of the diffraction maximum for the scattering of light from the probe wave a_0 into the cavity mode a_1 is the following: the atoms at all lattice sites scatter the light in phase with each other. For the plain standing or traveling waves, this condition means that in the expression for the operator $\hat{D}_{10}=\Sigma_{j=1}^K u_1^*(\mathbf{r}_j)u_0(\mathbf{r}_j)\hat{n}_j$, $u_1^*(\mathbf{r}_j)u_0(\mathbf{r}_j)=1$ for all sites j. Thus, $\hat{D}_{10}=\hat{N}_K$ is reduced to the operator of the atom number at K illuminated sites. In Eq. (7), after neglecting the dispersive frequency shift, the only statistical quantity is D_{10}^q giving the atom number at K sites for the configuration q. We will call this single statistical quantity as z: $D_{10}^q=z$, which varies between 0 and N reflecting all possible realizations of the atom number at K sites.

From Eq. (8), the light amplitudes in the diffraction maximum are proportional to the atom number z,

$$\alpha_z=Cz,\quad\text{with}\quad C=\frac{iU_{10}a_0}{(i\Delta_p-\kappa)}. \tag{14}$$

Thus, the probability to find the atom number z is given from Eq. (13) by

$$p(z,m,t)=z^{2m}e^{-z^2\tau}p_0(z)/\tilde{F}^2, \tag{15}$$

where we introduced the dimensionless time $\tau=2|C|^2\kappa t$ and new normalization coefficient $\tilde{F}$ such that $\Sigma_{z=0}^N p(z,m,t)=1$.

If the initial atom number z at K sites is uncertain, $p_0(z)$ is broad. For the SF state, the probability to find the atom number z at the lattice region of K sites is given by the binomial distribution [24],

$$p_{\mathrm{SF}}(z)=\frac{N!}{z!\,(N-z)!}\left(\frac{K}{M}\right)^z\left(1-\frac{K}{M}\right)^{N-z}. \tag{16}$$

For a lattice with the large atom and site numbers $N,M\gg1$ but finite N/M, it can be approximated as a Gaussian distribution,

$$p_{\mathrm{SF}}(z) = \frac{1}{\sqrt{2\pi}\sigma_z} e^{-(z-z_0)^2/2\sigma_z^2}, \tag{17}$$

with the mean atom number $\langle \hat{N}_K \rangle = z_0 = NK/M$ and $\sigma_z = \sqrt{N(K/M)(1-K/M)}$ giving the full width at a half maximum (FWHM) $2\sigma_z\sqrt{2\ln 2}$. The atom-number variance in the SF state is $(\Delta N_K)^2 = \langle \hat{N}_K^2 \rangle - \langle \hat{N}_K \rangle^2 = \sigma_z^2$.

Equation (15) shows how the initial distribution $p_0(z)$ changes in time. The function $z^{2m}\exp(-z^2\tau)$ has its maximum at $z_1 = \sqrt{m/\tau}$ and the FWHM $\delta z \approx \sqrt{2\ln 2/\tau}$ (for $\delta z \ll z_1$). Thus, multiplying $p_0(z)$ by this function will shrink the distribution $p(z,m,t)$ to a narrow peak at z_1 with the width decreasing in time.

Physically, this describes the projection of the atomic quantum state to a final state with the squeezed atom number at K sites (a Fock states $|z_1, N-z_1\rangle$ with the precisely known atoms at K sites z_1 and $N-z_1$ atoms at $M-K$ sites). Thus, the final quantum state of the light-matter system is

$$|\Psi_c\rangle = |z_1, N-z_1\rangle|\alpha_{z_1}\rangle, \tag{18}$$

which is a product state showing that the light and matter get disentangled. *A priori* z_1 is unpredictable. However, measuring the photon number m and time t, one can determine z_1 of the quantum trajectory.

Even the final Fock state (18) can contain the significant atom-atom entanglement, as this is still a many-body state. In general, the Fock state $|z_1, N-z_1\rangle$ cannot be factorized into the product of two states for K illuminated and $M-K$ unilluminated lattice sites. Thus, the entanglement can survive even between two lattice regions, which depends on the value of z_1 realized at a particular quantum trajectory. For some cases, the factorization is possible. For example (cf. Ref. [26]), the initial superfluid state after the measurement approaches the product of two superfluids: $|z_1, N-z_1\rangle = |\mathrm{SF}\rangle_{z_1,K}|\mathrm{SF}\rangle_{N-z_1,M-K}$.

Note that our model does not specify how K sites were selected, which is determined by the lattice and light geometry. The simplest case is to illuminate a continuous region. However, one can also illuminate each second site by choosing the probe wavelength twice as lattice period and get an atom-number squeezing at odd and even sites. In this way, one gets a measurement-prepared product of two SFs "loaded" at sites one by one (e.g., atoms at odd sites belong to one SF, while at even sites to another). While the initial SF, as usual, shows the long-range coherence $\langle b_i^\dagger b_j \rangle$ with the lattice period, the measurement-prepared state will demonstrate the doubled period in $\langle b_i^\dagger b_j \rangle$ (b_j is the atom annihilation operator such that $b_j^\dagger b_j = \hat{n}_j$). Thus, even though our model does not include the matter filed operators b_j but only the atom-number operators $\hat{n}_j$, the matter coherence can be still affected and modified by our QND measurement scheme in a nontrivial way.

The conditioned cavity photon number $\langle a_1^\dagger a_1 \rangle_c(t) = |C|^2 \Sigma_{z=0}^N z^2 p(z,m,t)$ is given by the second moment of $p(z,m,t)$. Finally, it reduces to $\langle a_1^\dagger a_1 \rangle_c = |C|^2 z_1^2$, reflecting a direct correspondence between the final atom number and cavity photon number, which is useful for the experimental measurements.

Further details of the light measurement at a diffraction maximum were presented in Ref. [26].

B. Preparation of the Schrödinger cat states

The macroscopic superposition state (Schrödinger cat state) can be prepared detecting light at the direction of a diffraction minimum [26]. The condition of the diffraction minimum for the scattering of light from the probe wave a_0 into the cavity mode a_1 is the following: the atoms at the neighboring lattice sites scatter the light with the phase difference π. For the plain standing or traveling waves, this condition means that in the expression for the operator $\hat{D}_{10} = \Sigma_{j=1}^K u_1^*(\mathbf{r}_j) u_0(\mathbf{r}_j)\hat{n}_j$, $u_1^*(\mathbf{r}_j)u_0(\mathbf{r}_j) = (-1)^{j+1}$. Thus, $\hat{D}_{10} = \Sigma_{j=1}^M (-1)^{j+1}\hat{n}_j$ is the operator of the atom-number difference between odd and even sites (in this subsection, we consider all sites illuminated $K=M$). Similarly to the previous subsection, in Eq. (7), after neglecting the dispersive frequency shift, the only statistical quantity is D_{10}^q giving the atom-number difference for the configuration q. We will call this single statistical quantity as z: $D_{10}^q = z$, which varies between $-N$ and N with a step 2 reflecting all possible realizations of the atom-number difference.

Equations (14) and (15) keep their form for the diffraction minimum as well, however, with a different meaning of the statistical variable z, which is now a realization of the atom-number difference, and $p(z,m,t)$ is its probability.

For the SF state, the probability to find the atom number at odd (or even) sites $\tilde{z}$ [$\tilde{z} = (z+N)/2$ because the atom-number difference is z and the total atom number is N] is given by the binomial distribution [24],

$$p_{\mathrm{SF}}(\tilde{z}) = \frac{N!}{\tilde{z}!\,(N-\tilde{z})!}\left(\frac{Q}{M}\right)^{\tilde{z}}\left(1-\frac{Q}{M}\right)^{N-\tilde{z}}, \tag{19}$$

where Q is the number of odd (or even) sites. For even M, $Q = M/2$ and Eq. (19) simplifies. For a lattice with the large atom and site numbers $N, M \gg 1$ but finite N/M, this binomial distribution—similarly to the previous subsection—can be approximated by a Gaussian function. Changing the variable as $z = 2\tilde{z} - N$, we obtain the Gaussian function for the probability to find the atom-number difference z,

$$p_{\mathrm{SF}}(z) = \frac{1}{\sqrt{2\pi}\sigma_z} e^{-(z^2/2\sigma_z^2)}, \tag{20}$$

with the zero mean z and $\sigma_z = \sqrt{N}$ giving the FWHM $2\sigma_z\sqrt{2\ln 2}$. The variance of the atom-number difference in the SF state is $\sigma_z^2 = N$.

The striking difference from the diffraction maximum is that our measurement and probability (15) are not sensitive to the sign of z, while the amplitudes $\alpha_z = Cz$ are. So, the final state obtained from Eq. (7) is a superposition of two Fock states with $z_{1,2} = \pm\sqrt{m/\tau}$ and different light amplitudes $\alpha_{z_2} = -\alpha_{z_1}$,

$$|\Psi_c\rangle = \frac{1}{\sqrt{2}}(|z_1\rangle|\alpha_{z_1}\rangle + (-1)^m|-z_1\rangle|-\alpha_{z_1}\rangle). \tag{21}$$

In contrast to a maximum, even in the final state, the light and matter are not disentangled. In principle, one can disen-

tangle light and matter by switching off the probe and counting all leaking photons. Then both $|\alpha_{z_1}\rangle$ and $|-\alpha_{z_1}\rangle$ will go to the vacuum $|0\rangle$. Thus, one can prepare a quantum superposition of two macroscopic atomic states $(|z_1\rangle+(-1)^m|-z_1\rangle)/\sqrt{2}$, which is a Schrödinger cat state that, in the notation of odd and even sites, reads as

$$\frac{1}{\sqrt{2}}\left(\left|\frac{N+z_1}{2},\frac{N-z_1}{2}\right\rangle+(-1)^m\left|\frac{N-z_1}{2},\frac{N+z_1}{2}\right\rangle\right).$$

We have shown that the detection of photons at the direction of a diffraction minimum leads to the preparation of Schrödinger cat state (21). The physical reason for this is that the quantum measurement of photons determines the absolute value of the atom-number difference $|z|$. However, as the photon number is not sensitive to the sign of z, one ends up in the superposition of states with the positive and negative values of z.

Unfortunately, Eq. (21) demonstrates a very strong disadvantage of such a method, which makes it difficult to realize experimentally. Each photodetection flips the sign between two components of the quantum superposition in Eq. (21). This means that if one loses even a single photocount, which is very probable for a realistic photodetector, one ends up in the mixture of two state (21) with plus and minus signs. Such a mixed state does not contain any atomic entanglement any more, in contrast to pure state (21), which is a highly entangled one.

Formally, the appearance of the sign flip $(-1)^m$ in Eq. (21) originates from Eq. (7), which contains the coefficient α_z^m in the prefactor of each Fock state. Since, in the final state, two components with opposite signs of light amplitudes survive $(\alpha_{z_2}=-\alpha_{z_1})$, the term α_z^m produces the coefficient $(-1)^m$. Therefore, even one photodetection changes the phase between two components in Eq. (21) by $\Delta\varphi_1=\pi$, which is the maximal possible phase difference. The idea to make the preparation scheme more stable with respect to the photon losses is based on the possibility to make this phase jump $\Delta\varphi_1$ smaller than π. In this case, losing one photon will also lead to the mixture of two cat states. However, if those cat states are not very different (i.e., the phase difference $\Delta\varphi_1$ is small), the mixed state will still contain significant atomic entanglement.

In Sec. VI, we present a scheme to prepare the Schrödinger cat state with a phase difference between two components smaller than π. Thus, such a scheme is more practical and robust with respect to the photon losses and, hence, decoherence.

The atom-number-squeezed state (18) prepared by observing light at a diffraction maximum is indeed more robust than the Schrödinger cat state (21) obtained at a diffraction minimum, as the former does not have any phase jump. However, the convenient property of the measurement at a minimum is that during the same time interval (e.g., during the shrinking time which is the same for a maximum and minimum, $\delta z\approx\sqrt{2\ln 2/\tau}$), the number of photons scattered at a diffraction minimum $(\langle a_1^\dagger a_1\rangle=|C|^2N)$ is much smaller than the one scattered at a maximum $(\langle a_1^\dagger a_1\rangle=|C|^2N_K^2)$ [23,25,26].

Further details of the light measurement at a diffraction minimum were presented in Ref. [26].

V. PHOTON STATISTICS

In this section, we consider three kinds of photon statistics: (i) statistics $p_\Phi(n,m,t)$ of the photon number n in a cavity after m photons were detected outside the cavity, (ii) statistics $P(m,t)$ of the photocount number m, and (iii) statistics $\tilde{P}_T(m,t)$ of the photocount number m if, after the time measurement T, m_T photons were detected.

First, let us consider the statistics of the number of photons in a cavity after the measurement time t and m photodetections. The joint probability to find a number of photons in a cavity n together with finding the atomic state in the Fock state $|q\rangle=|q_1,\ldots,q_M\rangle$ is obtained by projecting the general solution (6) on the state $|q\rangle|n\rangle$ and is given by

$$W_q(n,m,t)=\frac{|\alpha_q(t)|^{2n}}{n!}e^{-|\alpha_q(t)|^2}p_q(m,t),$$

where the probability to find the atomic Fock state $p_q(m,t)$ is given by Eq. (10). However, the probability to find n photons in a cavity independently of the atomic state is obtained by projecting solution (6) on the light Fock state $|n\rangle$ and taking the trace over the atomic states. Thus, the cavity photon number distribution function is given by

$$p_\Phi(n,m,t)=\sum_q\frac{|\alpha_q(t)|^{2n}}{n!}e^{-|\alpha_q(t)|^2}p_q(m,t),$$

where the sum is taken over all possible configurations q.

If, as in the previous section, the only atomic statistical quantity is z, the sum is simplified and the probability $p_\Phi(n,m,t)$ to find n photons in a cavity after the measurement time t and m photodetections reads as

$$p_\Phi(n,m,t)=\sum_z\frac{|\alpha_z(t)|^{2n}}{n!}e^{-|\alpha_z(t)|^2}p(z,m,t), \tag{22}$$

where the atom-number distribution $p(z,m,t)$ is given by Eq. (12).

In general, $p_\Phi(n,m,t)$ is a super-Poissonian distribution. During the measurement, the atomic distribution $p(z,m,t)$ shrinks to one or two symmetric peaks corresponding to the atom-number-squeezed or macroscopic superposition states. Thus, after some time, only a single term (or two equal terms) survives in the sum, and the cavity photon statistics $p_\Phi(n,m,t)$ evolves from super-Poissonian to Poissonian one. This fact can be checked experimentally.

During the measurement, the mean conditional photon number $\langle a_1^\dagger a_1\rangle_c$ approaches the value $|\alpha_{z_1}|^2$, which enables one to determine the final atom number z_1 by measuring the photon number in a cavity.

Let us now consider the probability $P(m,t)$ to detect m photons within the time t, if the initial atom-number distribution is $p_0(z)$. As shown, for example, in Ref. [59], this probability can be obtained from state (6) using the integration over all detection moments $t_1,t_2,\ldots,t_m$ from 0 to t (because we are not interested in the time moments, but only in

the total number of the photocounts m) and taking the trace. The simple result can be obtained for the case $t,t_1 > 1/k$ since solution (7) does not depend on the detection times. The probability reads as

$$P(m,t) = \sum_z \frac{(2\kappa|\alpha_z|^2 t)^m}{m!} e^{-2\kappa|\alpha_z|^2 t} p_0(z), \tag{23}$$

where the powers of m appear due to the m time integrations.

In contrast to the probability $p_\Phi(n,m,t)$ [Eq. (22)], which characterizes the conditional distribution of the cavity photons at a particular trajectory, the probability $P(m,t)$ depends on the initial atom-number distribution $p_0(z)$ and is not a characteristic of a particular quantum trajectory but rather of an ensemble average. In general, this is a super-Poissonian distribution, which does not approach any Poissonian one. From Eq. (23), the increase in the mean photocount number with time is given by

$$\langle m \rangle_0 = 2\kappa t \langle a_1^\dagger a_1 \rangle_0,$$

where $\langle a_1^\dagger a_1 \rangle_0$ is not a conditional photon number, but the one calculated for the initial atomic state. In average, the photocount number linearly increases in time. However, as the distribution is not Poissonian, the fluctuations of the photocount rate m/t do not decrease to zero.

One can also introduce another statistical distribution. The distribution $\tilde{P}_T(m,t)$ of the photocount number m if, after the measurement time T, m_T photons have been already detected. Similar approach, as in Eq. (23), leads to the following result:

$$\tilde{P}_T(m,t) = \sum_z \frac{[2\kappa|\alpha_z|^2(t-T)]^m}{m!} e^{-2\kappa|\alpha_z|^2(t-T)} p(z,m_T,T), \tag{24}$$

which, in contrast to Eq. (23), depends not on the initial atomic distribution, but on the distributuion at the time T. Thus, this probability combines the quantum trajectory evolution up to the time T and the ensemble average after that. As we know, the atomic distribution $p(z,m_T,T)$ approaches the single peak for the Fock state with increasing T. Therefore, this photocount probability approaches the Poissonian distribution with increasing T, the fluctuations of m grows in time as $\sqrt{m} \sim \sqrt{t}$, and the fluctuations of the photocount rate m/t vanishes with increasing time.

VI. STATE PREPARATION BY CAVITY TRANSMISSION MEASUREMENT

We now switch to a different probing scheme, using the probe through the mirror with the amplitude η (Fig. 1), and assuming no transverse probe $a_0=0$. From Eq. (8), we see that the light amplitudes depend only on the single statistical quantity $D_{11}^q = \Sigma_{j=1}^K |u_1(\mathbf{r}_j)|^2 q_j$, which reduces to the atom number at K sites for the traveling wave a_1 at any angle to the lattice, or for the standing wave a_1 with atoms trapped at the antinodes. Thus, in this case, the statistical quantity is $z = D_{11}^q$, which changes between 0 and N. The term $U_{11}D_{11}^q$ in Eq. (8) has a meaning of the dispersive frequency shift of the cavity mode due to the presence of atoms in a cavity.

The light amplitude α_z from Eq. (8) can be rewritten as a function of the atom number at K sites z,

$$\alpha_z = C' \frac{\kappa/U_{11}}{i(z-z_p)+\kappa/U_{11}} \quad \text{with} \quad C' = \frac{\eta}{\kappa}, \tag{25}$$

and the parameter $z_p = \Delta_p/U_{11}$ is fixed by the probe-cavity detuning Δ_p. The probability to find the atom number z (13) takes the form

$$p(z,m,t) = \frac{e^{-\tau'(\kappa/U_{11})^2/[(z-z_p)^2+(\kappa/U_{11})^2]}}{[(z-z_p)^2+(\kappa/U_{11})^2]^m} p_0(z)/F'^2, \tag{26}$$

where the dimensionless time is $\tau' = 2|C'|^2\kappa t$.

The prefactor function in front of $p_0(z)$ in Eq. (26) has a form more complicated than the one we had for the transverse probing in Eq. (15). However, it provides us a richer physical picture. In contrast to the transverse probing, this function allows us a collapse to both the singlet and doublet distributions. Thus, the measurement of the cavity transmission contains both cases of transverse probing at a diffraction maximum and minimum considered in Sec. IV.

If for a particular quantum trajectory the number of photocounts is large such that $m/\tau' \geq 1$, the distribution $p(z,m,t)$ collapses to a single-peak function at z_p. This singlet shrinks (FWHM) as $\delta z \approx 2(\kappa/U_{11})\sqrt[4]{2\ln 2/\tau'}$, which can be very fast for a high-Q cavity with the small κ. In the estimation of δz, we used the assumption that the peak has already become narrow, $\delta z \ll \kappa/U_{11}$, and that $m \approx 2\kappa\langle a_1^\dagger a_1 \rangle_c t$. Similar to the transverse probing, in the final state, the light and atoms are disentangled: $|z_p, N-z_p\rangle|\alpha_{z_p}\rangle$, which corresponds to the atom-number-squeezed (Fock) state and coherent light state.

If, however, the number of photocounts is small $m/\tau' < 1$, the distribution $p(z,m,t)$ collapses to a doublet centered at z_p with two satellites at $z_{1,2} = z_p \pm \Delta z$ with

$$\Delta z = \frac{\kappa}{U_{11}} \sqrt{\frac{\tau'}{m} - 1}. \tag{27}$$

When the doublet has become well separated (i.e., $\delta z \ll \Delta z$), each of its component shrinks in time as

$$\delta z \approx \Delta z \left(1 + \frac{\kappa^2}{U_{11}^2 \Delta z^2}\right) \sqrt{\frac{2\ln 2}{\tau'}\left(1 + \frac{U_{11}^2 \Delta z^2}{\kappa^2}\right)}.$$

Physically, tuning the probe at Δ_p, we may expect scattering from the atom number z_p providing such a frequency shift Δ_p. If the photocount number is large ($m/\tau' \geq 1$), indeed, the atom number is around z_p and it collapses to this value. However, if m is small, we gain knowledge that the atom number z is inconsistent with this choice of Δ_p, but two possibilities $z < z_p$ or $z > z_p$ are indistinguishable. This collapses the state to a superposition of two Fock states with $z_{1,2}$, symmetrically placed around z_p.

Thus, the transmission measurement scheme allows one to prepare both the atom-number-squeezed state and the Schrödinger cat state. The appearance of the singlet for squeezed state or the doublet for cat state can be determined by measuring m and t or the final photon number $\langle a_1^\dagger a_1 \rangle_c = |\alpha_{z_1}|^2$. From Eq. (25), we see that there is a direct corre-

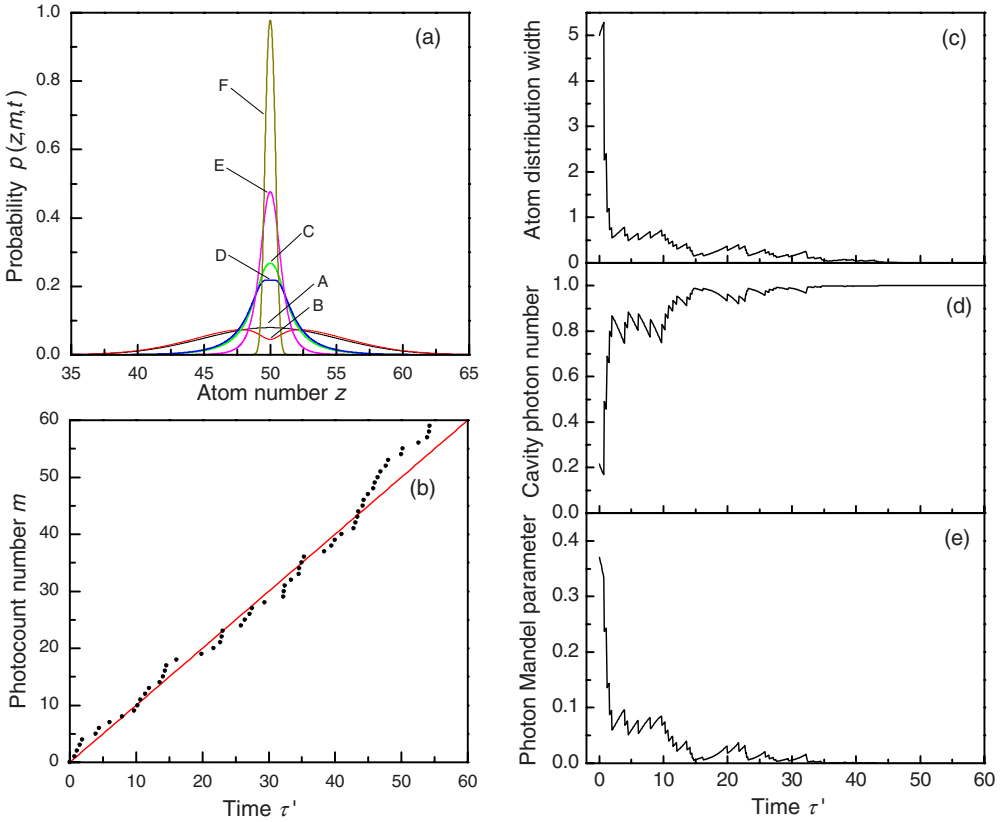

FIG. 2. (Color online) Photodetection trajectory leading to a single-peak distribution (atom-number squeezing). The probe-cavity detuning is chosen such that $z_p=50$ coincides with the initial distribution center. (a) Shrinking atom-number distribution at different times (A–F) $\tau'=0$ (number of photocounts is $m=0$), 0.7 (just before the first count, $m=0$), 0.7 (just after the first count, $m=1$), 1.1($m=1$), 1.1($m=2$), and 14.6($m=17$); (b) time dependence of the photocount number m, the red line is for $m=\tau'$; (c) decreasing width of the atom-number distribution; (d) reduced conditioned photon number $\langle a_1^\dagger a_1\rangle_c/|C'|^2$ with quantum jumps; and (e) photon Mandel parameter. Initial state: SF, $N=100$ atoms, $M=100$ lattice sites, and $K=M/2=50$ illuminated sites.

spondence between the final cavity photon number and the parameter of the doublet Δz,

$$\langle a_1^\dagger a_1\rangle_c = \frac{\eta^2}{U_{11}^2\Delta z^2+\kappa^2}, \tag{28}$$

which makes the experimental determination of the doublet position possible. The parameter Δz can be also determined by measuring the photocount number m and time t using Eq. (27).

In Figs. 2–5, we present the results, where the quantum trajectories of qualitatively different kinds were realized. In all figures, the initial state is the superfluid with the atom number $N=100$ at $M=100$ lattice sites; the half of all lattice sites $K=50$ are illuminated by the cavity mode. The initial distribution of the atom number at K sites is given by Eq. (16) and can be well approximated by the Gaussian distribution (17) with the mean value $\langle\hat{N}_K\rangle=z_0=NK/M=50$ and $\sigma_z=\sqrt{N(K/M)(1-K/M)}=5$.

Figure 2 presents the results for a quantum trajectory, which leads to the collapse to a single-peak distribution. In this case, the probe is detuned in such way that the probe-cavity detuning corresponds to the center of the atom-number distribution: $z_p=\Delta_p/U_{11}=50$. In Fig. 2(a), the evolution of the atom-number probability $p(z,m,t)$ [Eq. (26)] is shown. The curve A is the initial atom-number distribution having the Gaussian shape. Curve B shows the non-Hermitian evolution of the probability just before the first jump ($m=0$). As, at this time interval, the number of photocounts is small ($m/\tau'<1$), the distribution tends to a doublet. This is assured by the exponential factor in Eq. (26) leading to the suppression of the component at $z=z_p$ as one does not record the photocounts at the expected detuning. However, just after the photocount ($m=1$), this distribution instantly changes to the curve C, which has already a single peak as for this trajectory it turns out that $m/\tau'>1$. The switch to a single peak is assured by the Lorentzian factor in Eq. (26). After that, before the second jump, the probability decreases at $z=z_p$ and broadens (curve D) but jumps upward again and narrows, when the second jump occurs (curve E). Finally, after many jumps, the probability distribution becomes narrow and has a single peak at $z=z_p$ (curve F).

Figure 2(b) shows the number of photocounts m growing in time. It is clear that m stays always near the line $m=\tau'$. The appearance of the singlet is assured by the fact that at the initial stage $m/\tau'>1$.

Figure 2(c) shows the evolution of the width of the atom-number distribution $\sqrt{(\Delta N_K)^2}$, which decreases to zero reflecting the shrinking distribution. Figure 2(d) shows the reduced conditioned photon number in the cavity $\langle a_1^\dagger a_1\rangle_c/|C'|^2$.

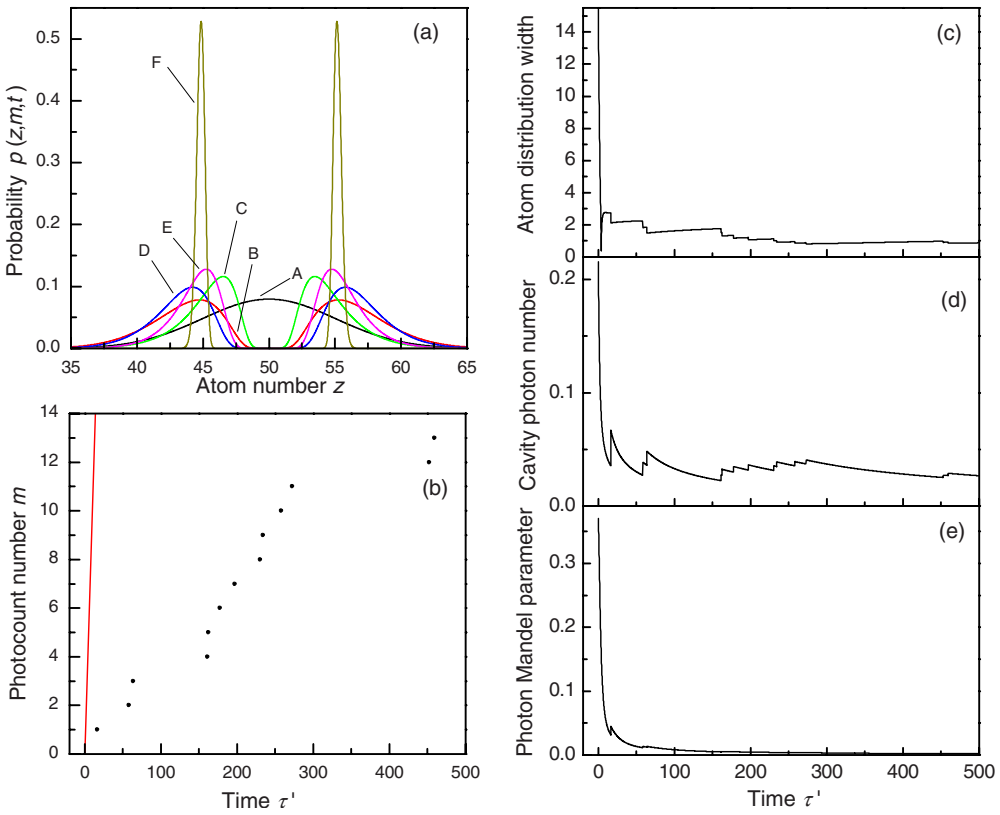

FIG. 3. (Color online) Photodetection trajectory leading to a doublet distribution (Schrödinger cat state). The probe-cavity detuning is chosen such that $z_p=50$ coincides with the initial distribution center. (a) Shrinking atom-number distribution at different times (A–F) $\tau'=0$ (number of photocounts is $m=0$), 16.4 (just before the first count, $m=0$), 16.4 (just after the first count, $m=1$), 58.2 ($m=1$), 58.2($m=2$), and 2017.6($m=73$); (b) time dependence of the photocount number m, the red line is for $m=\tau'$; (c) decreasing width of one of the peaks in the atom-number distribution; (d) reduced conditioned photon number $\langle a_1^\dagger a_1\rangle_c/|C'|^2$ with quantum jumps; and (e) photon Mandel parameter. Initial state: SF, $N=100$ atoms, $M=100$ lattice sites, and $K=M/2=50$ illuminated sites.

One sees that for the initial atom distribution, it starts from a relatively small value. However, as the atomic state goes to the Fock state with the atom number z_p exactly corresponding to the detuning Δ_p, it approaches the maximal possible value $\langle a_1^\dagger a_1\rangle_c/|C'|^2=1$. Moreover, one can easily see the quantum jumps in the initial stage, when the light field consists of several coherent-state components. Finally, the jumps disappear as the light state approaches a single coherent state $|\alpha_{z_p}\rangle$, when the atomic state approaches a Fock state. It is interesting to note that the photon escape from the cavity (photocount) leads to the increase in the conditional photon number in the cavity, while the no-count process leads to its decrease. This is a counterintuitive characteristic feature of the super-Poissonian photon statistics and is determined by the conditional nature of the probabilities considered [59]. Figure 2(e) shows the reduced Mandel parameter $Q/|C'|^2$ characterizing the photon number variance $Q=(\langle n_\Phi^2\rangle-\langle n_\Phi\rangle^2)/\langle n_\Phi\rangle-1$, where $n_\Phi=\langle a_1^\dagger a_1\rangle_c$ is the conditioned photon number. One can see how it decreases to zero corresponding to the coherent state of light. The parameters shown in Figs. 2(b)–2(e) can be measured experimentally, thus, presenting the verification of our theory.

Figure 3 presents the results for the case, where the detuning also corresponds to the atom-number distribution center $z_p=50$, but the quantum trajectory leads to the doublet distribution (Schödinger cat state). Figure 3(a) shows the evolution of the atom-number distribution $p(z,m,t)$. Curve A is the initial Gaussian distribution. Before the first jump (curve B), the distribution evolves to a doubletlike, similar to the curve B in Fig. 2(a). However, in contrast to Fig. 2(a), the first photocount does not return the distribution back to the single peak and it stays doubletlike (curve C). This is so because the first jump occurs rather late such that $m/\tau'<1$. Next jumps are rather late as well, so the distribution evolves to a doublet (curves D–F).

Figure 3(b) shows the number of photocounts m growing in time. It is clear that, in contrast to Fig. 2(b), m is always much smaller than the line $m=\tau'$ (red line), which gives the experimental possibility to claim the appearance of the doublet.

Figures 3(c)–3(e), similarly to Fig. 2, show the decrease in the width of one of two peaks of the atom-number distribution, conditioned cavity photon number with disappearing jumps, and the Mandel parameter approaching zero. Note that in contrast to Fig. 2(d), the conditioned photon number $\langle a_1^\dagger a_1\rangle_c/|C'|^2$ does not approach the maximal value 1 but rather decreases to a smaller value given by the doublet splitting Δz [Eq. (28)]. Thus, the appearance of the doublet can be characterized by experimentally measuring m and t [Fig. 3(b)] or the cavity photon number [Fig. 3(d)].

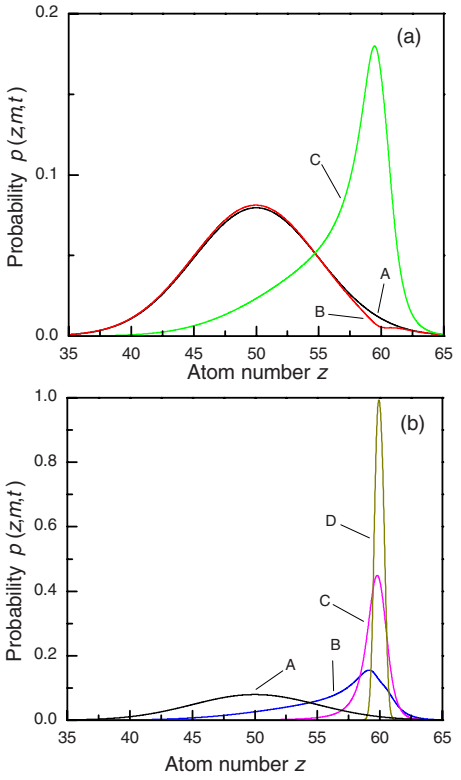

FIG. 4. (Color online) Photodetection trajectory leading to a single-peak distribution (atom-number squeezing). The probe-cavity detuning is chosen such that $z_p=60$ is at the wing of the initial distribution. Shrinking atom-number distribution at different times (A–C) (a) $\tau'=0$ (number of photocounts is $m=0$), 0.7 (just before the first count, $m=0$), and 0.7 (just after the first count, $m=1$); (b) (A–D) $\tau'=0(m=0)$, $1.1(m=1)$, $1.1(m=2)$, and 14.6 $(m=17)$. Initial state: SF, $N=100$ atoms, $M=100$ lattice sites, and $K=M/2=50$ illuminated sites.

Figures 4 and 5 present another situation, where the probe-cavity detuning is chosen such that $z_p=60$, which corresponds to a wing of the atomic distribution function.

Figure 4 shows the evolution of the atom-number distribution in case, where it collapses to a singlet at z_p. Thus, here even the conditioned mean atom number changes from 50 to $z_p=60$. Other characteristics of this process look very similar to the ones presented in Figs. 2(b)–2(e).

Figure 5 shows the collapse to a doublet distribution around $z_p=60$ with $\Delta z=7$. Thus, two satellites in Fig. 5(a) are placed at $z_1=67$ and $z_2=53$. However, while the satellite at $z_2=53$ is near the maximum of the initial distribution and is well seen, the second satellite at $z_1=67$ falls on the far wing and is practically invisible. As a result, the final distribution looks as a singlet at $z_2=53$, while the second satellite is very small. The fact that one has indeed a doublet can be verified by measuring the photocount number [Fig. 5(b)], which is obviously less than τ', or by measuring the cavity photon number [Fig. 5(e)], which is less than the maximal value 1 and depends on Δz. The measurement of the mean atom number [Fig. 5(c)] or width of atomic distribution [Fig. 5(d)] would not distinguish between the singlet and doublet.

This suggests us a method to prepare the macroscopic superposition state with unequal amplitudes of two components. Choosing the detuning Δ_p such that z_p is not at the center of the initial atom-number distribution, one can expect that one of the satellites will be very probable near the distribution center, while another one will fall on its wing.

The most important difference of the Schrödinger cat state prepared by the transmission measurement from the one prepared by transverse probing (21) is that the phase difference between two components of the quantum superposition is not limited by the values of 0 and π as in Eq. (21). Although the light amplitudes corresponding to z_1 and z_2 has equal absolute values, their phases are opposite: $\alpha_{z_1}=|\alpha_{z_1}|\exp(i\varphi)$ and $\alpha_{z_2}=|\alpha_{z_1}|\exp(-i\varphi)$, where from Eq. (25) the light phase φ is

$$\varphi=-\arctan\frac{U_{11}\Delta z}{\kappa}. \tag{29}$$

Moreover, the imaginary parts of the functions Φ_q in Eqs. (7) and (9) are also different for z_1 and z_2 and have opposite signs: $\Phi(t)=\mathrm{Im}\,\Phi_{z_1}(t)=-\mathrm{Im}\,\Phi_{z_2}(t)=\mathrm{Im}(\eta\alpha_{z_1}^*)$. Using Eq. (25),

$$\Phi(t)=|\alpha_{z_1}|^2U_{11}\Delta z t. \tag{30}$$

Thus, using Eq. (7), the cat state is given by

$$|\Psi_c\rangle=\frac{1}{F'}[e^{im\varphi+i\Phi(t)}|z_1\rangle|\alpha_{z_1}\rangle\sqrt{p_0(z_1)} + e^{-im\varphi-i\Phi(t)}|z_2\rangle|\alpha_{z_2}\rangle\sqrt{p_0(z_2)}], \tag{31}$$

which is a macroscopic superposition of two Fock states with the atom numbers z_1 and z_2 at K sites.

Using the probe-cavity detuning Δ_p, one can choose the center of the doublet $z_p=\Delta_p/U_{11}$. Moreover, Eq. (31) shows that using this detuning one can influence, at least—probabilistically—the ratio between two components in superposition (31). In particular, if we tune the probe frequency such that z_p coincides with the center of the initial atom-number distribution $p_0(z)$, the probabilities of the symmetric doublet components will be equal $[p_0(z_1)=p_0(z_2)]$, providing the equal amplitudes of the cat components in Eq. (31).

The phases $\Phi(t)$ and $m\varphi$ have opposite evolution in time. The phase term $\Phi(t)$ [Eq. (30)] grows in time linearly and deterministically, while the term $m\varphi$ grows in time stochastically according to the growth of the photodetection number m. In average, $\langle m\rangle=2\kappa|\alpha_{z_1}|^2t$. Thus, in general, the phase difference between two cat components grows in time linearly. However, for some parameters, the growth of the average $\langle m\rangle\varphi$ and $\Phi(t)$ can be compensated. From Eqs. (29) and (30), $\langle m\rangle\varphi+\Phi(t)=0$ for $U_{11}\Delta z/\kappa\approx 2.33$. So, for the particular cat components, the phase difference does not grow in average. However, as m is a stochastic quantity, its uncertainty grows in time as $\sqrt{t}$ (cf. Sec. V). Thus, the phase difference will still grow in time as $\sqrt{t}$, which is, however, much slower than the linear growth.

The problem of photon losses addressed in the previous section is related to the stochastic quantity $m\varphi$. A single photocount changes the phase difference between two components by $\Delta\varphi_1=2\varphi$. In contrast to state (21), where the phase jump is always maximal $\Delta\varphi_1=\pi$, here, this jump can be rather small, if the condition $U_{11}\Delta z/\kappa<1$ is fulfilled. This

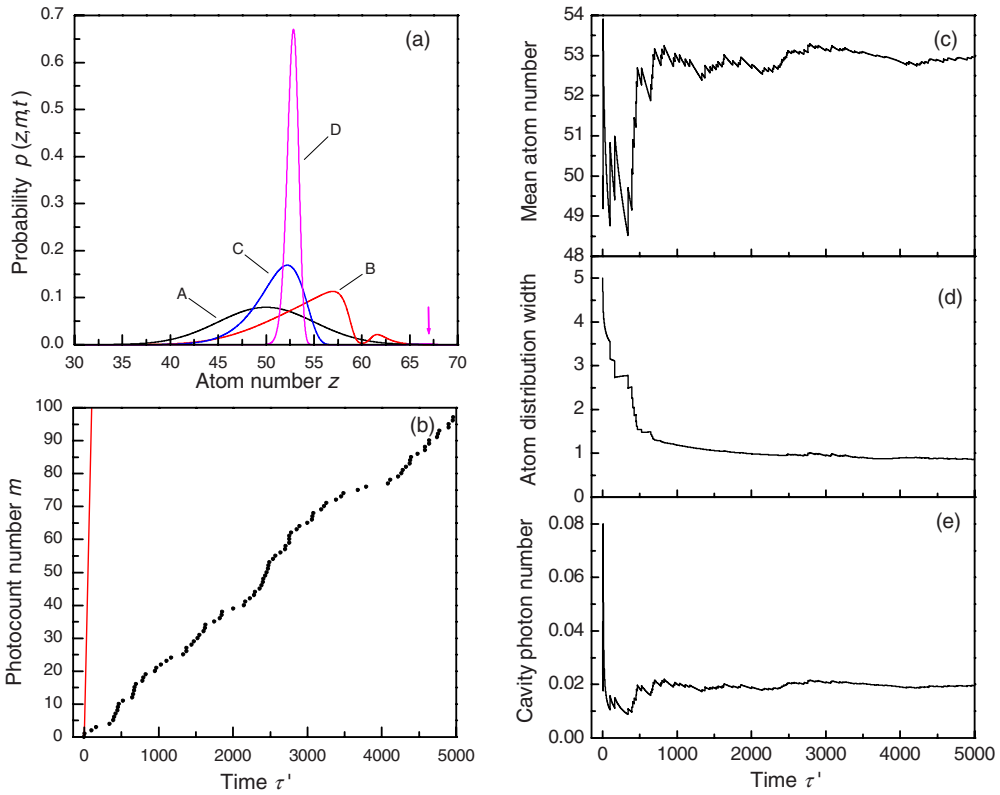

FIG. 5. (Color online) Photodetection trajectory leading to a doublet distribution (Schrödinger cat state). The probe-cavity detuning is chosen such that $z_p=60$ is at the wing of the initial distribution. (a) Shrinking atom-number distribution at different times (A–D) $\tau'=0$ (number of photocounts is $m=0$), 5.4($m=1$), 163.5($m=3$), and 2006.9($m=39$); the arrow shows the position of the very small doublet component, which is almost invisible; (b) time dependence of the photocount number m, the red line is for $m=\tau'$; (c) conditioned mean atom number; (d) decreasing width of the atom-number distribution; and (e) reduced conditioned photon number $\langle a_1^\dagger a_1\rangle_c/|C'|^2$ with quantum jumps. Initial state: SF, $N=100$ atoms, $M=100$ lattice sites, and $K=M/2=50$ illuminated sites.

means that to provide the robustness of the state with respect to the photon losses, the doublet should not be split too strongly. In the next section, we quantitatively analyze the robustness of the cat state.

VII. ROBUSTNESS OF THE SCHRÖDINGER CAT STATES

The macroscopic superposition state (31) is a pure state. In principle, if the measurement is perfect and all photons m leaking the cavity are counted by a photodetector, it will evolve according to Eq. (31) staying pure. However, if one loses one or more photons, the state becomes a mixture of several states corresponding to several lost counts l. Thus, if L photons are lost, the state is a mixture of $L+1$ states of the following form for $0<l<L$:

$$|\Psi_c\rangle_l=\frac{1}{\sqrt{2}}[e^{il\varphi+i\gamma}|z_1\rangle|\alpha_{z_1}\rangle+e^{-il\varphi-i\gamma}|z_2\rangle|\alpha_{z_2}\rangle], \tag{32}$$

where, for simplicity, we assumed the symmetric superposition with $p_0(z_1)=p_0(z_2)$ and included all known phases [for m measured photons and deterministic $\Phi(t)$] into the term $\gamma=m\varphi+\Phi(t)$. The density matrix of state (32) is

$$\rho_l=\frac{1}{2}(|z_1\rangle|\alpha_{z_1}\rangle\langle z_1|\langle\alpha_{z_1}|+|z_2\rangle|\alpha_{z_2}\rangle\langle z_2|\langle\alpha_{z_2}|+e^{i2l\varphi+i2\gamma}|z_1\rangle|\alpha_{z_1}\rangle \times\langle z_2|\langle\alpha_{z_2}|+e^{-i2l\varphi-i2\gamma}|z_2\rangle|\alpha_{z_2}\rangle\langle z_1|\langle\alpha_{z_1}|). \tag{33}$$

The density matrix of the mixture state describing L lost photons is given by a sum of density matrix (33),

$$\rho^{(L)}=\frac{1}{2}\Bigg(|z_1\rangle|\alpha_{z_1}\rangle\langle z_1|\langle\alpha_{z_1}|+|z_2\rangle|\alpha_{z_2}\rangle\langle z_2|\langle\alpha_{z_2}| +\frac{e^{i2\gamma}}{L+1}\sum_{l=0}^{L}e^{i2l\varphi}|z_1\rangle|\alpha_{z_1}\rangle\langle z_2|\langle\alpha_{z_2}| +\frac{e^{-i2\gamma}}{L+1}\sum_{l=0}^{L}e^{-i2l\varphi}|z_2\rangle|\alpha_{z_2}\rangle\langle z_1|\langle\alpha_{z_1}|\Bigg). \tag{34}$$

The quantity characterizing how close is a mixture state to a pure state is the so-called purity $P=\mathrm{Tr}(\rho^2)$. For a pure state, it is maximal and equal to 1, while for a maximally mixed state it is minimal and equal to 1/2 (in our case of the two-component states). The purity of state (34) is given by

$$P_L = \frac{1}{2}\left[1 + \frac{1}{(L+1)^2}\left|\sum_{l=0}^{L} e^{i2l\varphi}\right|^2\right], \tag{35}$$

where the sum can be calculated leading to the following result for the purity of the mixed state corresponding to L lost photons:

$$P_L = \frac{1}{2}\left[1 + \frac{1}{(L+1)^2}\frac{\sin^2(L+1)\varphi}{\sin^2\varphi}\right]. \tag{36}$$

For example, in the simplest case, where one photon is lost, the density matrix of the mixed state is given by the sum of two terms (33) with $l=0$ and 1,

$$\rho^{(1)} = \frac{1}{2}\Big(|z_1\rangle|\alpha_{z_1}\rangle\langle z_1|\langle\alpha_{z_1}| + |z_2\rangle|\alpha_{z_2}\rangle\langle z_2|\langle\alpha_{z_2}| + \frac{1}{2}e^{i2\gamma}(1+e^{i2\varphi}) \times |z_1\rangle|\alpha_{z_1}\rangle\langle z_2|\langle\alpha_{z_2}| + \frac{1}{2}e^{-i2\gamma}(1+e^{-i2\varphi})|z_2\rangle|\alpha_{z_2}\rangle\langle z_1|\langle\alpha_{z_1}|\Big), \tag{37}$$

which has a purity

$$P_1 = \frac{1}{2}(1+\cos^2\varphi) = \frac{1}{2}\left(1 + \frac{1}{1+(U_{11}\Delta z/\kappa)^2}\right). \tag{38}$$

Equations (37) and (38) show that if the phase jump associated with the one-photon lost $\Delta\varphi_1 = 2\varphi$ is maximal $\Delta\varphi_1 = \pi$, state (37) is maximally mixed because all nondiagonal terms responsible for the quantum coherence between the states $|z_1\rangle|\alpha_{z_1}\rangle$ and $|z_2\rangle|\alpha_{z_2}\rangle$ are zero. Its purity (38) is 1/2, thus no entanglement survived after the single photon lost. This is a situation of the transverse probing in the diffraction minimum [Eq. (21)], where the phase jump is π, which makes the preparation scheme practically difficult.

However, if φ is small, purity (38) and the nondiagonal coefficients in Eq. (37) can be rather large and close to 1. Thus, after the photon has been lost, one gets a mixed state but that of the high purity. More generally, for L photon losses, Eqs. (34) and (36), the total phase jump $\Delta\varphi_L = 2L\varphi$ should be small. Using the expression for φ Eq. (29), one can estimate the condition for the high purity of the mixed state as $\varphi < \pi/(2L)$, which for a small φ is approximately the condition $U_{11}\Delta z/\kappa < \pi/(2L)$. As a result, for the doublet, which is split not too strongly, the high purity can be preserved even with photon losses.

The purity (36) as a function of the doublet splitting Δz for $L=0$, 1, 3, and 10 photon losses is shown in Fig. 6, where φ is given by Eq. (29). One can see the decrease in the purity with increasing doublet splitting and number of photons lost. Note the nonmonotonous character of its decrease, which means that the larger splitting does not automatically leads to a smaller purity.

VIII. CONCLUSIONS

We explicitly calculated the quantum state reduction induced by measurement of off-resonant-scattered light from an ultracold quantum gas trapped in an optical lattice. In our previous papers [23–25], the expectation values of various

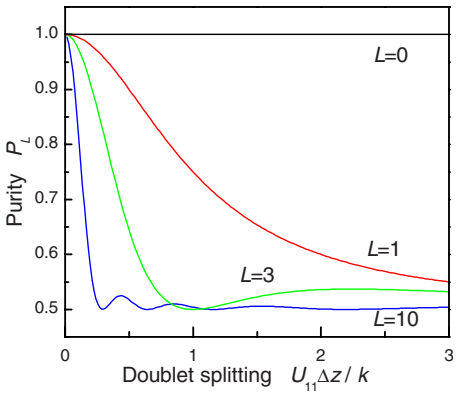

FIG. 6. (Color online) Purity of the mixed state as a function of the doublet splitting Δz for different numbers L of the photocounts lost: $L=0$, 1, 3, and 10.

atomic and light quantities were analyzed, thus, assuming the repeated measurement to enable the averaging procedure. In contrast, in this paper, we were focused on a single run of the optical measurement, i.e., the evolution of the quantities at a single-quantum trajectory. As the scattered light is entangled to the atoms, quantum backaction of the light measurement alters the atomic state. The geometry, which determines the form of entanglement, thus dictates the possible measurement results and final atomic states.

Any quantum state related to an eigenstate of the weighted atom-number operators $\hat{D}_{lm}$ can thus be prepared in a probabilistic way. The type of the states can be chosen by the optical geometry and their probabilities are determined from the initial distribution. Typically, light detection at the diffraction maximum leads to the preparation of the atom-number-squeezed states, while the detection at a minimum prepares the macroscopic superposition states peaked at a pair of atom numbers.

The robustness of the resulting Schrödinger cat states with respect to undetected photons was analyzed. The transmission measurement scheme was shown to prepare the states more robust than the ones prepared by the detection at a diffraction minimum.

In contrast to recent results in spin squeezing and preparation of the spin superposition states, which can be also obtained for thermal atoms [30,44–48], in our work, the quantum nature of ultracold atoms is crucial, as we deal with the atom-number fluctuations appearing due to the delocalization of ultracold atoms in space.

We demonstrated the time evolution of various measurable quantities appearing exclusively due to the measurement procedure (as other obvious sources of dynamics, such as tunneling, were neglected). The quantum dynamics is governed by the quantum jumps and conditional evolution. The quantum state preparation is probabilistic. However, it can be generalized by including the feedback loop, which will enable the quasideterministic state preparation. In this case, the trapping potential should be continuously modified depending on the outcome of the photodetector. For example, the detection of photons at a diffraction maximum squeezes the atomic number at K sites around some value z_1, which was

not known *a priori*. The potential can be continuously tilted in a way to provide the increase or decrease in this atom number to enable ones to obtain the number squeezed state with a mean value $\tilde{z}_1$ given *a priori*. The same method can be applied for the atom-number squeezing at odd or even sites.

Our results can be applied for other quantum arrays as well, e.g., ion strings [55], and be useful for the preparation of various atomic and photonic multipartite entangled states [60]. Moreover, they can have a relation to the problem of interaction of ultracold atoms with other bosonic particles besides photons [61,62].

Cavity QED with quantum gases can operate with the atom numbers ranging from millions to one [63]. Thanks to the recent experimental breakthroughs [6–9], preparing various kinds of atom-number squeezing is already doable, and the creation of—at least—small-amplitude Schrödinger cat states [64,65] may become practical.

ACKNOWLEDGMENT

This work was supported by the Austrian Science Fund FWF (Grants No. P17709 and No. S1512).

[1] I. Bloch, J. Dalibard, and W. Zwerger, Rev. Mod. Phys. **80**, 885 (2008).
[2] M. Lewenstein *et al.*, Adv. Phys. **56**, 243 (2007).
[3] M. Scully and S. Zubairy, *Quantum Optics* (Cambridge University Press, New York, 1997).
[4] D. Jaksch, C. Bruder, J. I. Cirac, C. W. Gardiner, and P. Zoller, Phys. Rev. Lett. **81**, 3108 (1998).
[5] M. Greiner, O. Mandel, T. Esslinger, T. Hänsch, and I. Bloch, Nature (London) **415**, 39 (2002).
[6] F. Brennecke *et al.*, Nature (London) **450**, 268 (2007).
[7] Y. Colombe *et al.*, Nature (London) **450**, 272 (2007).
[8] S. Slama, S. Bux, G. Krenz, C. Zimmermann, and P. W. Courteille, Phys. Rev. Lett. **98**, 053603 (2007).
[9] F. Brennecke *et al.*, Science **322**, 235 (2008).
[10] M. G. Moore, O. Zobay, and P. Meystre, Phys. Rev. A **60**, 1491 (1999).
[11] H. Pu, W. Zhang, and P. Meystre, Phys. Rev. Lett. **91**, 150407 (2003).
[12] L. You, M. Lewenstein, and J. Cooper, Phys. Rev. A **51**, 4712 (1995).
[13] Z. Idziaszek, K. Rzazewski, and M. Lewenstein, Phys. Rev. A **61**, 053608 (2000).
[14] Ö. E. Müstecaplioğlu and L. You, Phys. Rev. A **62**, 063615 (2000).
[15] Ö. E. Müstecaplioğlu and L. You, Phys. Rev. A **64**, 033612 (2001).
[16] J. Javanainen, Phys. Rev. Lett. **75**, 1927 (1995).
[17] J. Javanainen and J. Ruostekoski, Phys. Rev. A **52**, 3033 (1995).
[18] J. I. Cirac, M. Lewenstein, and P. Zoller, Phys. Rev. Lett. **72**, 2977 (1994).
[19] J. I. Cirac, M. Lewenstein, and P. Zoller, Phys. Rev. A **50**, 3409 (1994).
[20] H. Saito and M. Ueda, Phys. Rev. A **60**, 3990 (1999).
[21] G. A. Prataviera and M. C. de Oliveira, Phys. Rev. A **70**, 011602(R) (2004).
[22] J. Javanainen and J. Ruostekoski, Phys. Rev. Lett. **91**, 150404 (2003).
[23] I. B. Mekhov, C. Maschler, and H. Ritsch, Phys. Rev. Lett. **98**, 100402 (2007).
[24] I. B. Mekhov, C. Maschler, and H. Ritsch, Nat. Phys. **3**, 319 (2007).
[25] I. B. Mekhov, C. Maschler, and H. Ritsch, Phys. Rev. A **76**, 053618 (2007).
[26] I. B. Mekhov and H. Ritsch, Phys. Rev. Lett. **102**, 020403 (2009).
[27] I. B. Mekhov and H. Ritsch, Laser Phys. **19**, 610 (2009).
[28] W. Chen, D. Meiser, and P. Meystre, Phys. Rev. A **75**, 023812 (2007).
[29] W. Chen and P. Meystre, Phys. Rev. A **79**, 043801 (2009).
[30] K. Eckert *et al.*, Nat. Phys. **4**, 50 (2008).
[31] A. B. Bhattacherjee, Opt. Commun. **281**, 3004 (2008).
[32] J. Ruostekoski, J. Javanainen, and G. V. Dunne, Phys. Rev. A **77**, 013603 (2008).
[33] J. M. Zhang, W. M. Liu, and D. L. Zhou, Phys. Rev. A **77**, 033620 (2008).
[34] I. de Vega, J. I. Cirac, and D. Porras, Phys. Rev. A **77**, 051804(R) (2008).
[35] L. Guo, S. Chen, B. Frigan, L. You, and Y. Zhang, Phys. Rev. A **79**, 013630 (2009).
[36] C. Maschler and H. Ritsch, Phys. Rev. Lett. **95**, 260401 (2005).
[37] C. Maschler, I. B. Mekhov, and H. Ritsch, Eur. Phys. J. D **46**, 545 (2008).
[38] J. Larson, B. Damski, G. Morigi, and M. Lewenstein, Phys. Rev. Lett. **100**, 050401 (2008).
[39] J. Larson, S. Fernandez-Vidal, G. Morigi, and M. Lewenstein, New J. Phys. **10**, 045002 (2008).
[40] A. Vukics, C. Maschler, and H. Ritsch, New J. Phys. **9**, 255 (2007).
[41] A. Vukics, W. Niedenzu, and H. Ritsch, Phys. Rev. A **79**, 013828 (2009).
[42] D. Nagy, G. Szirmaia, and P. Domokos, Eur. Phys. J. D **48**, 127 (2008).
[43] G. Szirmai, D. Nagy, and P. Domokos, Phys. Rev. Lett. **102**, 080401 (2009).
[44] J. Hald, J. L. Sorensen, C. Schori, and E. S. Polzik, Phys. Rev. Lett. **83**, 1319 (1999).
[45] D. Meiser, J. Ye, and M. J. Holland, New J. Phys. **10**, 073014 (2008).
[46] C. Genes and P. R. Berman, Phys. Rev. A **73**, 013801 (2006).
[47] A. E. B. Nielsen and K. Molmer, Phys. Rev. A **77**, 052111 (2008).
[48] A. E. B. Nielsen, U. V. Poulsen, A. Negretti, and K. Molmer, Phys. Rev. A **79**, 023841 (2009).
[49] H. Zoubi and H. Ritsch, Phys. Rev. A **79**, 023411 (2009).
[50] M. Brune, S. Haroche, J. M. Raimond, L. Davidovich, and N. Zagury, Phys. Rev. A **45**, 5193 (1992).

[51] Y. P. Huang and M. G. Moore, Phys. Rev. A **73**, 023606 (2006).
[52] J. Ruostekoski, M. J. Collett, R. Graham, and D. F. Walls, Phys. Rev. A **57**, 511 (1998).
[53] J. F. Corney and G. J. Milburn, Phys. Rev. A **58**, 2399 (1998).
[54] D. A. R. Dalvit, J. Dziarmaga, and R. Onofrio, Phys. Rev. A **65**, 033620 (2002).
[55] W. M. Itano, J. C. Bergquist, J. J. Bollinger, J. M. Gilligan, D. J. Heinzen, F. L. Moore, M. G. Raizen, and D. J. Wineland, Phys. Rev. A **47**, 3554 (1993).
[56] H. Carmichael, *An Open System Approach to Quantum Optics* (Springer-Verlag, Berlin, 1993).
[57] T. Yu. Ivanova and D. A. Ivanov, Opt. Commun. **272**, 148 (2007).
[58] C. W. Gardiner and P. Zoller, *Quantum Noise* (Springer-Verlag, Berlin, 1999).
[59] M. Ueda, N. Imoto, H. Nagaoka, and T. Ogawa, Phys. Rev. A **46**, 2859 (1992).
[60] D. Porras and J. I. Cirac, Phys. Rev. A **78**, 053816 (2008).
[61] M. Bruderer, A. Klein, S. R. Clark, and D. Jaksch, Phys. Rev. A **76**, 011605(R) (2007).
[62] A. Klein and D. Jaksch, EPL **85**, 13001 (2009).
[63] P. Maunz *et al.*, Nature (London) **428**, 50 (2004).
[64] A. Ourjoumtsev *et al.*, Science **312**, 83 (2006).
[65] J. S. Neergaard-Nielsen, B. M. Nielsen, C. Hettich, K. Molmer, and E. S. Polzik, Phys. Rev. Lett. **97**, 083604 (2006).